Simulation of Hybrid PV Solar System with Fuel Cell in MATLAB Simulink

FERNANDA REMACHE, JESSICA CASTILLO, CARLOS QUINATOA, LUIS CAMACHO
Department of Electrical Engineering,
University Technical of Cotopaxi,
Av. Simón Rodríguez s/n Barrio El Ejido Sector San Felipe,
ECUADOR

Abstract: - This paper discusses the simulation of a fuel cell hybrid solar photovoltaic system in MATLAB Simulink. To achieve the stated objective, it is proposed to dynamically model a hybrid system using Simulink to analyze its performance and optimize its operation, improving the efficiency and stability of the power supply under different operating conditions, then the dynamic simulation model employs energy conversion equations of the solar PV panel and the fuel cell to meet the electrical load requirements, where the solar panel uses solar radiation and ambient temperature, while the fuel cell produces electricity by electrolysis of water, which separates hydrogen from oxygen. In the first graph, the power at load increases sharply at 0.5 seconds and stabilizes between 0.5 and 1.5 seconds, with a sharp drop at 1.6 seconds. In the second graph, PV power increases at 0.5 seconds, reaching 80 kW between 0.5 and 1.5 seconds, dropping to zero at 1.6 seconds. The fuel cell shows similar behavior. These results indicate a coordinated operation for a stable power supply to the load, responding efficiently to changes in demand and generation.

Key-Words: - Problems, Workers, Radiation, Electromagnetic, Electric.

Received: April 18, 2024. Revised: August 23, 2024. Accepted: September 21, 2024. Published: October 29, 2024.

1 Introduction

Renewable energy sources are essential to mitigate the environmental impacts associated with traditional energy sources. Several studies highlight the positive results of renewable energy on the environment, such as reducing pollution, fighting global warming and combating climate change, [1]. However, it is essential to evaluate the environmental impacts of renewable energy projects themselves, with a specific focus on wind and solar energy as primary sources. While energy installations can pose challenges to aesthetics, ecosystems, and public health, solar energy stands out for its minimal adverse environmental effects. In addition, [2], [3], academic research emphasizes the influence of transitioning to renewable sources of energy to address issues related to economic progress, greenhouse gas emissions, and the advancement of sustainable economies in middle- and high-income countries, [4].

Renewable energies, such as solar panels and fuel cells, are vital elements of sustainable energy production. Solar panels harness sunlight to produce electricity, representing a renewable and environmentally friendly source of energy, [5]. In cases of insufficient sunlight, fuel cells act as supplementary energy sources, ensuring uninterrupted power supply and system reliability, [6]. The integration of solar panels and fuel cells in hybrid systems improves the efficiency of energy production and reduces the environmental impact by avoiding the emission of harmful substances and using renewable sources, [7]. In addition, fuel cells can store surplus energy from solar panels by generating hydrogen through electrolysis, allowing energy to be stored and used during periods of low sunlight. This partnership between solar panels and fuel cells embodies a sustainable strategy to meet energy demands while addressing environmental concerns.

Increasing energy demand and the urgency to decrease greenhouse gas emissions have driven the advancement of renewable energy systems. Hybrid systems, which combine solar PV with other sources such as fuel cells, are gaining importance due to their ability to provide a more reliable and efficient power supply. However, the complexity associated with integrating and monitoring these systems requires advanced simulation tools to evaluate their functionality and improve their efficiency. MATLAB Simulink is presented as a robust platform for modeling and simulation of dynamic systems, including renewable energy systems.

To address these difficulties, it has been proposed to integrate hybrid systems that combine solar PV with alternative generation sources, such as fuel cells. Merging these two technologies into a hybrid system has the potential to fix the stability and efficiency of energy supply. Although, the inclusion of multiple energy sources brings additional complexities in system design, monitoring and operation.

Improving these hybrid systems requires advanced simulation tools that can accurately replicate the dynamic performance of each component and their interactions.

Simulation of a hybrid solar PV system with a fuel cell in MATLAB Simulink presents a promising approach to address the growing energy demand while mitigating environmental impact. The integration of solar power and fuel cells enables the establishment of a reliable and efficient power generation configuration, [5]. The predominant use of photovoltaic panels for power generation, supplemented by backup fuel cells during periods of low sunlight or peak demand, ensures a constant power supply, [8], [9]. The addition of a fuel cell allows energy storage to be utilized during non-generation periods, which improves system reliability and meets various load requirements, [7]. Through simulations performed in MATLAB Simulink, the efficiency and performance of these hybrid systems can be thoroughly evaluated and improved, demonstrating their potential for sustainable energy production.

The performance of the solar photovoltaic hybrid fuel cell system involves the integration of solar panels and fuel cells to provide a consistent and environmentally friendly energy source for domestic use. Typically, this hybrid configuration comprises a photovoltaic array, a fuel cell, an electrolyzer and power control units, [10]. During the day, the solar panels harness solar energy to generate electricity, while the fuel cell batteries use hydrogen produced through the electrolysis of water from the solar panels to produce energy in low light conditions or at night, [11]. System efficiency can range from 1.75% to 7.66%, depending on variables such as current density and overall system design, [11]. By combining these technologies and including energy storage solutions such as supercapacitors, this hybrid system ensures a reliable and uninterrupted power supply for residential energy consumption, improving the intelligence and energy efficiency of the home.

The efficiency of a hybrid solar photovoltaic fuel cell system exceeds that of traditional energy sources, illustrating a promising approach to clean energy generation and utilization. By combining photovoltaics (PV) and hydrogen fuel cells (FC), these integrated systems can achieve impressive operating efficiencies, [11], with an overall efficiency of up to 47.9%, significantly higher than typical energy sources. Harnessing sustainable sources of energy such as solar and wind, together with energy technologies such as hydrogen photovoltaic fuel cells (HPF), presents a viable solution to the world's energy dilemma by lowering costs and improving reliability in power generation, [12]. The integration of photovoltaic and PV technologies not only improves efficiency, but also helps reduce greenhouse gas emissions, making it a sustainable and environmentally friendly energy production alternative for the future, [13].

Model and dynamically simulate a fuel cell hybrid solar PV system using MATLAB Simulink to analyze its performance and optimize its operation, improving the efficiency and stability of the power supply under various operating conditions.

2 Dynamic Model of Fuel Cell Hybrid Solar Photovoltaic Solar System

This chapter is structured in several sections, each of which addresses the specific cell types to be used and the corresponding formulas for determining the voltage, current, power and efficiency of solar PV panels, fuel cells and hybrid systems.

2.1 PEM type fuel cell

PEM batteries use hydrogen as a fuel and oxygen as oxidizer to facilitate the chemical reaction that generates electrons. These electrons then flow through an external electrical circuit, resulting in the production of water as a by-product of the process. This particular type of battery system is widely recognized for its environmentally sustainable characteristics, [14].

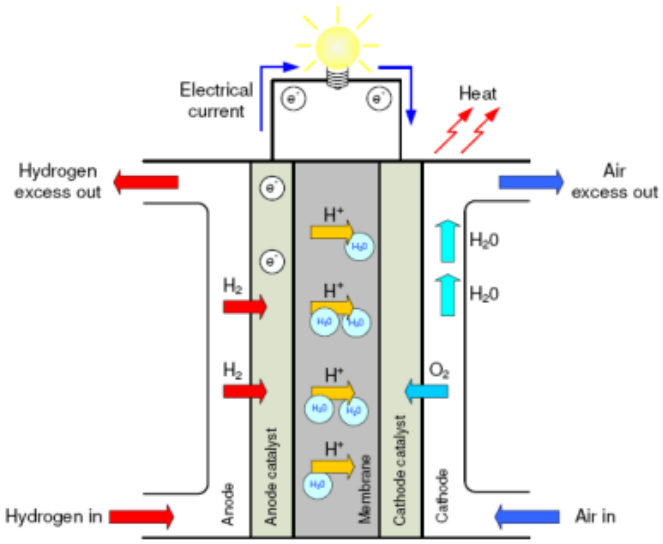

Fig. 1: PEM fuel cell design

Figure 1 shows the general performance of a fuel cell, showing the input of fuel, such as hydrogen, on the anode side, and the input of the oxidant, oxygen, on the cathode side, [15]. At the anode, the electron separates from the hydrogen atom and, following an external electrical circuit, moves through the

charge until it reaches the cathode. Meanwhile, the hydrogen atoms travel through the electrolyte to combine with the oxygen atom, resulting in the production of wastewater. This process generates heat, with temperatures ranging from 20 °C to 100 °C, highlighting the additional benefit of heat generation.

2.2 Photovoltaic solar panel system

Each of the equations used to perform the dynamic modeling of the hybrid solar PV/fuel cell system is described below.

Solar photovoltaic panels are composed of modules, and each module contains arrays and cells. Equation 1 must be used to achieve a dynamic current output, [16].

$$I = N_p * I_{ph} - N_p * I_o * \left[exp\left(\frac{\frac{U}{N_s} + I * \frac{R_s}{N_p}}{n * V_t} \right) - 1 \right] - I_{sh} \quad (1)$$

The parameter N_p represents the number of cells connected in parallel, while N_s indicates the number of cells connected in series. The variable U indicates the voltage of each individual cell. To determine the actual photo I_{ph}, it is essential to use equation 2, [16].

$$I_{ph} = [I_{sc} + K_i(T - 298)] * \frac{I_r}{1000} \quad (2)$$

I_{sc} is the abbreviation of the short-circuit current expressed in amperes (A). K_i indicates the short-circuit current of the cell under standard test conditions at 25 °C with a solar irradiance of 1000 W/m². T represents the operating temperature measured in Kelvin (K), while I_r represents the solar irradiance in units of watts per square meter (W/m²).

To obtain the current saturation I_{rs}, equation 3 introduced by [16], should be used.

$$I_{rs} = \frac{I_{sc}}{\left[exp(\frac{qV_{oc}}{N_s K_n T}) - 1 \right]} \quad (3)$$

The electronic charge q, denoted 1.16x10^{-19} C, is a fundamental constant. The open circuit voltage, V_{oc}, is a crucial parameter in electrical circuits. The ideality factor of the diode, represented by n, plays an important role in its performance. Boltzmann's constant, denoted K and equal to 1.3805 x 10^{-23} J/K, is essential in statistical mechanics.

The saturation current of the I_o module changes with cell temperature. Equation 4 is used to determine this current, [16], [17].

$$I_o = I_{rs} \left[\frac{T}{T_r} \right]^3 exp\left[\frac{q * E_{go}}{nk} \left(\frac{1}{T} - \frac{1}{T_r} \right) \right] \quad (4)$$

The location of I_{rs} has been identified as corresponding to equation 3, where T_r represents the nominal temperature set at 298.15 K, and E_{go} indicates the broadband energy of the semi-conductor, which is equivalent to 1.1 e_V.

To determine the current I_{sh}, information on the series resistance R_s and shunt resistance R_{sh} in ohms, along with the diode thermal voltage, must be possessed. Subsequently, equation 5 is used once these parameters have been identified, [16].

$$I_{sh} = \frac{\frac{N_p}{N_s} + I * R_s}{R_{sh}} \quad (5)$$

Once the asset current of the PV solar panel I (I_{pv}) is established, the power can be calculated by applying Ohm's law (equation 6).

$$P_{pv} = I_{pv} * V_{pv} \quad (6)$$

The value of V_{pv} is set according to the specifications provided in the data sheet of the solar PV panel.

To evaluate the efficiency of the solar PV system, a crucial step is to have a clear understanding of the input power Q_{in}, which is determined by equation 7 described by [18].

$$Q_{in} = I_r * S_p * \alpha_{abs} \quad (7)$$

The solar irradiance in W/m² is denoted as I_r, while the area of the solar PV panel is represented by S_p, and α_{abs} represents the overall absorption coefficient.

By acquiring the powers Q_{in} and P_{pv}, the efficiency can be determined using equation 8, [18].

$$\eta_{pv} = \frac{Q_{in}}{P_{pv}} \quad (8)$$

2.3 Theoretical model of PEM fuel cell system

For measuring the voltage of a fuel cell, a first step is to analyze the dynamic model. Research in the field of PEM fuel cell articles has been ongoing for many years. As a result, models that have been presented in advance will be used.

To convert the excess solar energy generated into hydrogen, it is essential that the electrolyzer matches the power output of the solar photovoltaic panels.

To determine the hydrogen production rate, equation 9 described by [19], is used.

$$x_H = 5,18 * e^{-6} * I_e \quad (9)$$

When x_H is expressed in moles/s, I_e represents the electric current flowing through the electrode terminals.

To determine the energy content represented by hydrogen, equation 10 should be used for its calculation, [19].

$$E_{H2} = \frac{Load}{\eta_{FC}} \tag{10}$$

The load represents the upper and lower limits of energy storage in kilowatt-hours (kWh), while $_{FC}$ indicates the fuel cell efficiency, calculated using equation 10.

Once the amount of energy stored in hydrogen is identified, it is essential to establish the corresponding mass of hydrogen m_{H2} associated with this energy. To achieve this, the gross calorific value (GCV) of the hydrogen molecule is used using equation 11, [19].

$$m_{H2} = \frac{E_{H2}}{PCS_{H2}} \tag{11}$$

The GCV of hydrogen is 142 MJ/kg or 39.4 kW/h. In equation 11, it is given as PCS_{H2} and the mass of hydrogen is quantified in kg/sec.

At a temperature of 15 °C and an atmospheric pressure of 1 atm (1.013 bar full), the thickness of hydrogen is calculated to be 0.085 kg/m³. Using this density value, the volume of hydrogen (V_{H2}) can be determined by applying equation 12, [19].

$$V_{H2} = \frac{m_{H2}}{0,085} \tag{12}$$

In m_{H2} is the mass of hydrogen calculated above with equation 11.

Gas compression systems are often identified as significant power consumers. By using Equation 13, the amount of compression power required to compress a gas from an inlet pressure $Pe_{(atm)}$ to an outlet pressure $Ps_{(atm)}$ can be calculated, [19].

$$P_{comp} = \frac{q_{gas}T_eC_p}{\eta_c}\left((\frac{P_s}{P_e})^{\frac{\gamma-1}{\gamma}} - 1\right) \tag{13}$$

The symbol q_{gas} represents the mass flow rate of the kg/s, specifically hydrogen. T_e indicates the access temperature of the gas, which is measured in Kelvin (K). C_p represents the calorific value of the gas (J/kg.k). The symbol η_c stands for the efficiency of the compressor output. Finally, γ represents the isentropic gas coefficient.

Using equation 14, the compression energy E_{comp} can be determined, [19].

$$E_{comp} = Mass*\frac{\gamma-1}{\gamma}\frac{P_eV_o}{\eta_c}\left((\frac{P_s}{P_e})^{\frac{\gamma-1}{\gamma}} - 1\right) \tag{14}$$

The mass of hydrogen can be given as mass in kg/s, while the initial volume of the gas is represented by V_o. In the specific hydrogen scenario, the initial volume is calculated as 11.11 m³/kg.

The theoretical framework of a PEM is presented below to obtaining voltage, power and efficiency acquisition. The transport of protons across the membrane and electrons through the external circuit generates a voltage disparity between the fuel cell terminals.

The stress produced can be determined by equation 15, [20]

$$U_s = U_{th} - U_{act} - U_{ohm} - U_{conc} \tag{15}$$

The theoretical U_{th} stress is determined using equation 16 in this model, which requires consideration of temperature variations with respect to the reference temperature, [20] .

$$U_{th} = 1,2297+(T-298,15)\frac{\Delta S_o}{nF}+\frac{RT}{nF}ln\left(\frac{P_{h2}P_{o2^{1/2}}}{P_{o^{1/3}}}\right) \tag{16}$$

The operating temperature of the cell indicated by T, S_o represents the change in reaction entropy of liquid water under standard test conditions, with a value of -0.1634 kJ/k/mol. The variable *n* represents the number of electrons by mole (n = 2), while *F* indicates the Faraday constant (96485.309 C/mol) and *R* represents the universal gas constant (8,31451 J/k/mol).

To determine the transient voltage, which variations with time, it is essential to use equation 17 for the calculation, [21].

$$U_{act} = \frac{dV_{act}}{dt} = \frac{I_s}{C} - \frac{U_{act}}{\frac{R_a}{C}} \tag{17}$$

The location of I_s is associated with the current (A), while C represents a fixed value of 108.75 F and, finally, there is an activation resistance R_a. To determine R_a, one must use equation 18 and have information on the decrease of the activation voltage η_{act} and I_s in relation to the current, [21].

$$R_a = \frac{-\eta_{act}}{I_s} \tag{18}$$

Equation 19 is applicable in cases where there is a decrease in the activation voltage, [22].

$$\eta_{act} = 0,9514 + 0,00312T - 0,000187T\,ln(i)+ 7,4x10^{-5}T\ln(C_{o2}) \tag{19}$$

The temperature of the fuel cell, denoted as T in kelvin, correlates closely with the temperature of the cell. The static current through the stack, represented

as i (A), and the dissolved oxygen concentration, denoted C_{o2}, are determined by equation 20, [22].

$$C_{o2} = \frac{P_{o2}}{5,08x10^6 exp\left(\frac{-498}{T}\right)} \tag{20}$$

The oxygen pressure on the cathode side is indicated as P_{o2}, while the temperature is represented by the symbol T.

By determining the voltage at U_s, it is possible to calculate the power output of the fuel cell by applying Ohm's law (equation 21):

$$P_{pc} = I_{pc} * U_s \tag{21}$$

The I_{pc} value is set according to the specifications provided by the fuel cell manufacturer.

To evaluate the efficiency of the η_{pv} fuel cell, equation 22 is used.

$$\eta_{stack} = 0,83 * \frac{U_s}{U_{th}} \tag{22}$$

2.4 Model of charge controller

The output power of the charge controller is usually defined by equation 23, [18], [23], [24].

$$P_{Cont-dc} = V_{Bat}\left(I_{rect} + I_{PV} + I_{FC}\right) \tag{23}$$

V_{Bat} represents the product of the nominal DC voltage of a given system, while I_{rect} indicates the rectifier output current. I_{PV} indicates the current produced by the solar photovoltaic panels, and I_{FC} stands for the current produced by the fuel cell.

2.5 Battery charging and discharging model

The batteries are responsible for accumulate the surplus energy regulated by the charge controller (Figure 2). In addition, their function includes monitoring voltage levels to ensure that they remain within the specified range, thus avoiding excessive discharges and preventing overcharging.

During the charging period, the correlation between voltage and current is represented by equation 24, [23].

$$V = V_r + \frac{I(\frac{0,189}{1,142-soc+R_i})}{AH} + (soc - 0,9)\,ln\left(300\frac{I}{AH} + 1,0\right) \tag{24}$$

The value of V_r is calculated using equation 25.

$$V_r = 2,94(1,0 - 0,001(T - 25°C)) \tag{25}$$

Battery current, indicated as I, represents the flow of electrical charge in amperes. Ah, which stands for ampere-hour, quantifies the total charge capacity of the battery as it discharges, soc or state of charge, indicates the proportion of charge being used at a specific time relative to the maximum charge capacity.

However, equation 26 is used for the discharge cycle, [23].

$$V = V_r + \frac{I}{AH} + \frac{0,189}{soc} + R_i \tag{26}$$

The internal resistance of the cell, indicated as R_i, and the ambient temperature, represented by T, are considered in the determination of R_i by establishing equation 27.

$$R_i = 0,15(1,0 - 0,02(T - 25°C)) \tag{27}$$

2.6 Inverter model

The characteristics are defined by the input power of the inverter and the output power it delivers. Inverters invariably incur losses during the conversion process, which underscores the importance of considering the manufacturer's specifications, [25].

Equation 28 is used to calculate the output inverter power.

$$P_{inv-ip}\eta_{inv} = P_{inv-op} \tag{28}$$

2.7 Hybrid system efficiency

Ultimately, the energy conversion efficiency of solar PV panels and fuel cell systems is determined by applying equation 29.

$$\eta_{sh} = (P_{pv} + P_{pc})/(I_r * S_p) \tag{29}$$

2.8 General flow diagram

The schematic diagram presented in Figure 2 shows the sequential progression within each numerical iteration of the dynamic simulation model designed for the hybrid system. These iterations correspond to equations 1 to 29, as described in chapter three.

The process begins with the input of the essential parameters required for the calculation. These parameters include Ir, which represents the radiation in W/m², T, which indicates the ambient temperature, I, which represents the rated current, and V, which represents the rated voltage of the solar PV panel, as distributed by the manufacturer. She represents the area of the solar PV panel, along with fuel cell-related parameters such as I and V, among others. Once the input of these parameters is finalized, each of the aforementioned equations is solved sequentially, starting from equation 1 to equation 8. This sequence

allows the extraction of energy from the solar PV panel system. Moving on to equations 9 through 22, the calculation involves determining the power output of the fuel cell, which encompasses the energy conversion process for hydrogen mass determination and energy storage. Equation 23 is dedicated to obtaining power from the charge controller. In addition, equations 24 to 27 provide information on the loading and unloading voltage of the system batteries. Equation 28 facilitates the calculation of the alternating current for the system, while equation 29 evaluates the efficiency of the hybrid method.

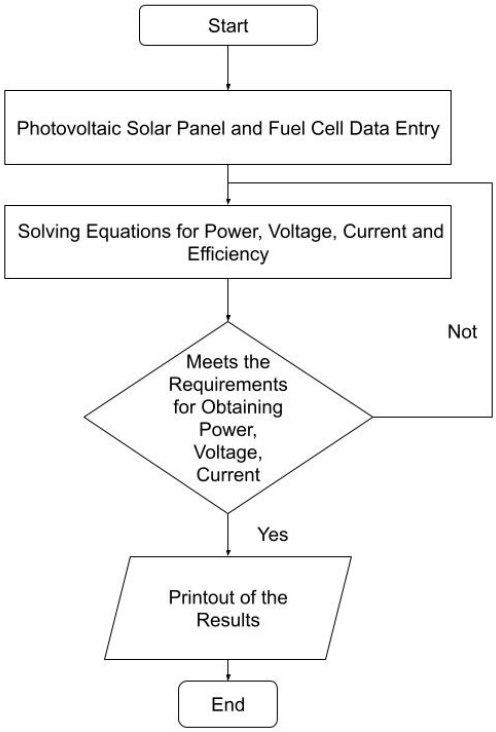

Fig. 2: Flow diagram of the calculation system

3 Validation of a Hybrid Photovoltaic and Fuel Cell Method

This chapter presents the results of simulations performed within the program, illustrating various voltage curves, current trends, load variations, efficiency levels and other relevant data through screenshots.

Figure 3 shows the fundamental components of a hybrid solar PV panel and fuel cell system. In this schematic, the interconnection of each component is depicted, starting with the solar PV panel linked to the charge controller, which establishes a connection between the battery bank and one of its terminals. A main capacity of the charge controller is to protect the battery bank against overcharging by maintaining a specific voltage level at its terminal.

In cases where there is a sudden voltage surge that exceeds the current threshold allowed for the load, the load will shed; as both current and voltage normalize, it is reconnected, similar to the process observed when current is at a minimum in the PV solar panel.

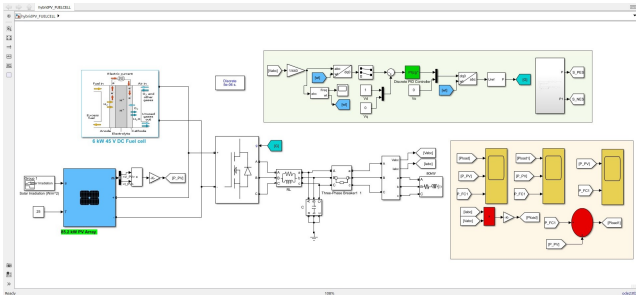

Fig. 3: PEM fuel cell design

The system consists of the following:

- 6 kW Fuel Cel
- 85.2 KW PV Solar System
- 80 KW
- 100 KW Inverter with controller based on PI Controller.

The system supplies from 0.5 seconds to 1.5 seconds.

3.1 Fuel cell general data

To facilitate the fuel cell simulation, additional subsystems must be integrated to monitor the fuel cell behavior. This includes the incorporation of a gas supply system and a Boost converter with RL load, operating at a constant voltage of 100 V, as shown in Figure 4. The simulink block is equipped with predefined outputs that allow observing various parameters of the fuel cell, such as efficiency, gas consumption, flow ratio, composition, Tafel curve slope, exchange current, Nernst voltage, open circuit voltage, as well as voltage and current, [26].

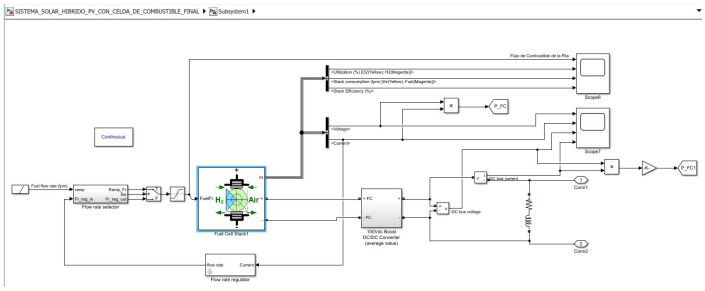

Fig. 4: Diagram of the PEM type cell

Simulink incorporates three PEM-type fuel cell stacks that are precharged to power levels of 1.26 kW, 6 kW, and 50 kW. The 6 kW battery was chosen to be used for this particular scenario as detailed in Table 1 with its corresponding parameters.

Table 1. Parameters of the 6 kW fuel cell stack

Fuel Cell Stack Parameters	
Battery power rating	5998.5 W
Maximum battery power	8325 W
Fuel cell resistance	0.07833 Ω
Single cell Nerst voltage (E_n)	1.1288 V
Nominal use of H_2	99.56 %
Nominal utilization O_2	59.3 %
Nominal fuel consumption	60.38 SLPM
Nominal air consumption	143.7 SLPM
Exchange current (i_o)	0.29197
Exchange ratio (α)	0.60645
Fuel composition (x_{H_2})	99.95 %
Oxidant Composition (y_{O_2})	21 %
Ratio of nominal fuel flow to utilization H_2 nominal	50.06 LPM
Maximum fuel flow ratio at nominal utilization (H_2)	84.5 LPM
Maximum air flow ratio at nominal utilization of (O_2)	506.4 LPM
System temperature (T)	338 K
Fuel feed pressure (P_{Fuel})	1.5 bar
Air supply pressure (P_{Fair})	1 bar

3.2 General solar panel data

A PV field is established by implementing strings of PV section connected in parallel, as shown in detail in Table 2 below.

Table 2. Data of PV array

PV array	
Parallel strings	40
Modules linked in series through a chain	20
Module data	
Maximum Power (W)	213.15
Open circuit voltage Voc (V)	36.3
Voltage at maximum power point Vmp (V)	29
Temperature coefficient of Voc $(\%/deg.C)$	-0.36099
Cells per module (Ncell)	60
Short-circuit current Isc (A)	7.84
Current at maximum power point Imp (A)	7.35
Temperature coefficient of Isc $(\%/deg.C)$	0.102
T cell (deg. C)	45-25
Model parameters	
Light-generated current IL (A)	7.8654
Diode saturation current I0 (A)	2.9273e-10
Diode ideality factor	0.98119
Shunt resistance Rsh (ohms)	313.0553
Series resistance Rs (ohms)	0.39381

Each string is composed of section connected in series, which allows modeling a series of predefined PV modules present in the model, together with user-defined PV modules.

It is essential to reach the required power of 213.15 W, for which a total of 10 panels with a power of 85.2 kW each are modeled. The solar cell is adjusted according to the specifications provided in the technical documentation of the solar panel. A radiation profile is formulated based on the ambient solar conditions, and specific sensors to measure current and voltage are strategically placed inside a singular unit that houses the 10 panels.

Figure 5 shows two graphs: the first graph illustrates the current-voltage (I-V) characteristics, while the second graph illustrates the power-voltage (P-V) characteristics of a photovoltaic (PV) array at two different temperatures: 25 °C and 45 °C.

Top graph: Current-voltage characteristics (I-V)

- The short circuit current (I_{SC}) remains constant at both temperatures (25 °C and 45 °C), approximately 320 A, suggesting minimal (I_{SC}) variation with temperature. The open circuit voltage (V_{OC}) is higher at 25 °C (about 700 V) than at 45 °C (about 640 V). The reduction of (V_{OC}) with increasing temperature is attributed to the reduction of the energy band gap in semi-conductor materials. The I-V curve presents the typical profile of a PV module: constant current at lower voltages and a sharp decrease near the (V_{OC}). At 45 °C, the curve shifts towards lower voltages compared to 25 °C.

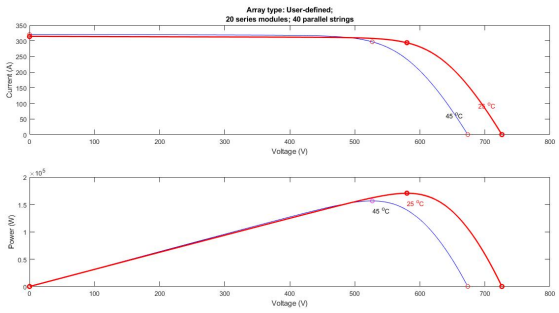

Fig. 5: Solar panel diagram

- The maximum power point (MPP) at 25 °C is placed at a higher voltage level (about 600 V) and has a higher power output compared to the (MPP) at 45 °C, which is placed at a lower voltage (about 550 V). This observation suggests that the temperature increase leads to a reduction in both voltage and maximum output power. The maximum power generated at 25 °C is high (approximately 2 x 10 ^ 5 W) compared to the maximum power at 45 °C, which is slightly lower. It is observed that the efficiency and

power output of the PV modules decrease with increasing temperature. The P-V curve shows a linear progression from 0 to its maximum point, followed by a sudden decrease, which occurs at a lower voltage at the highest temperature (45 °C) than at the lowest (25 °C).

3.3 Model applied to hybrid system

The show depicts a block diagram that may constitute a segment of a hybrid PV system incorporating a fuel cell. This diagram shows the correlation between currents, voltages within a three-phase system and load power. In the context of a hybrid PV system with a fuel cell, this diagram could exemplify the calculation of the instantaneous or average power delivered to a specific load. Hybrid systems combine various energy sources to ensure an uninterrupted and reliable power supply. This scheme is often used to monitor and regulate the power flow within these systems. Figure 6 below shows the details:

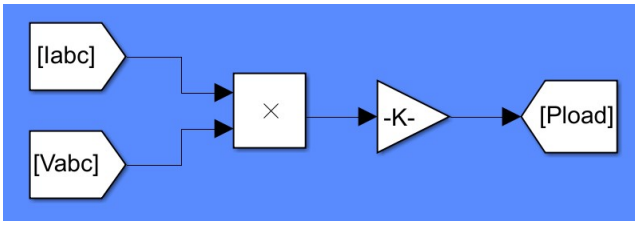

Fig. 6: Load power calculation

In this model, we observe a mathematical model in which the total load power of the panel is determined. This calculation includes the current I_{abc} and voltage V_{abc}, with the application of a specific gain of 0.001 for total efficiency.

The block diagram depicted in Figure 7 is a component of a hybrid photovoltaic system incorporating a fuel cell. This schematic delineates the merging of the power outputs derived from these sources.

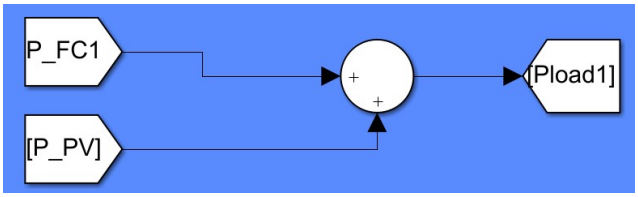

Fig. 7: Total power calculation

In the schematic, the P_{FC1} input represents the power output of the fuel cell, while the P_{PV} input represents the power output of the PV system. These power outputs are aggregated by an adder block (+), and the resulting output [Load1] indicates the total power supplied to the load, which comprises the accumulated power from both sources.

In the context of a hybrid PV system integrating a fuel cell, this scheme serves to elucidate how power outputs from various energy sources are combined to ensure a constant and reliable supply. Hybrid systems take advantage of multiple energy sources to compensate for each other's various limitations.

3.4 Load demand of PV Array

Figure 8 shows three graphs showing the power distributed to the load, the energy generated by the photovoltaic panel (PV Power) and the energy produced by the fuel cell (Fuel Cell Power). A review of each graph is presented below:

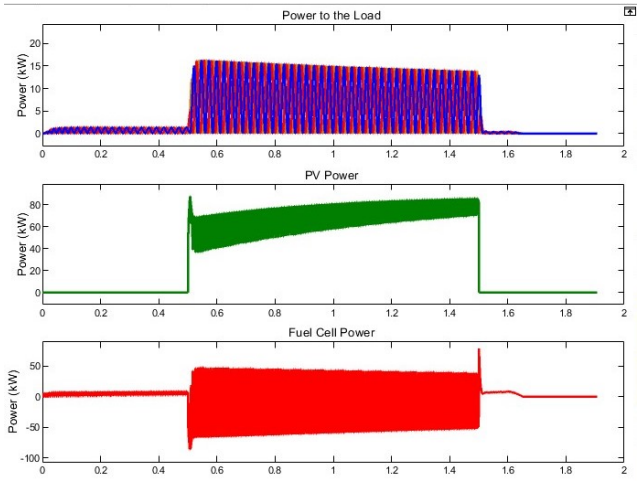

Fig. 8: Load demand of PV Array

Power to the Load:

- The ability to supply power to the load is shown in the graph, which shows variations over time. There is a noticeable increase in power around the 0.5 point on the x-axis, followed by a stabilization phase with recurring variations. These variations appear to be due to variations in power generation or load consumption.

PV Power:

- The power output of the PV panel starts from zero and subsequently undergoes a rapid increase close to 0.5 on the x-axis. After this initial increase, the power output stabilizes until it reaches 1.5 on the x-axis, at which point it drops sharply to zero. This observation suggests that the PV panel produces power steadily for a defined period before stopping its generation.

Fuel Cell Power:

- The fuel cell power starts at a negative level, which could indicate an initial power consumption. At about point 0.5 on the x-axis,

there is a sudden change and the power remains consistently negative until point 1.5 on the x-axis, where it changes back to a value close to zero. This pattern of behavior implies that the fuel cell is adjusting to variations in power generation from the PV array to ensure a constant supply of power to the load.

Together these graphs show the dynamic interaction between the PV array and the fuel cell to meet the load demand. It appears that the fuel cell serves as a key element in ensuring the stability of the power supplied to the load amidst variations in PV power output.

3.5 Load demand, PV array and fuel cell power

Figure 9 shows three graphs showing the relationship between power and time in a hybrid power generation system incorporating photovoltaic (PV) panels and fuel cells. The graphs specifically show the power supplied to the load, the power produced by the PV panels, and the power generated by the fuel cells. A subsequent analysis of each of the graphs is performed.

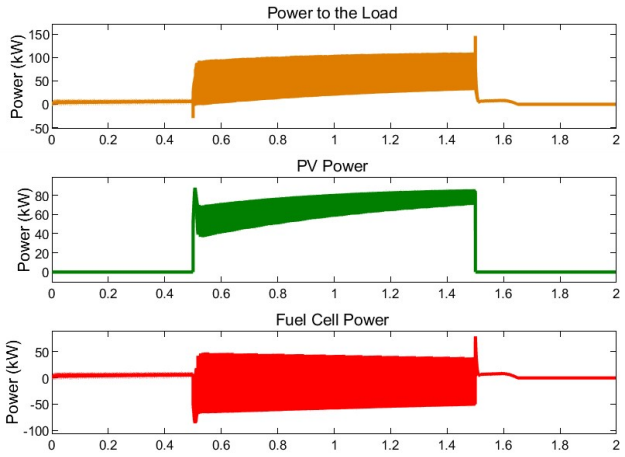

Fig. 9: Hybrid system load demand

Power supplied to the load:

- The x-axis of the graph shows the time in seconds (from 0 to 2 seconds), while the y-axis represents the power in kW (from -50 to 150 kW). Initially, the load power remains stable at a low level. At about 0.5 seconds, there is a sudden increase in power consumption, which reaches a maximum of about 75 kW. From 0.5 to 1.5 seconds, there is a continuous increase in power. At about 1.6 seconds, there is a sharp drop in power, which returns to a low, but positive value.

Photovoltaic array power (PV):

- The graph shows the time in seconds (0 to 2 seconds) on the x-axis and the power in kW (0 to 80 kW) on the y-axis. At the beginning, the PV panel generates no power. A sudden increase in power occurs around 0.5 seconds, with a maximum of about 25 kW. From 0.5 to 1.5 seconds, there is a gradual increase in PV power up to about 80 kW. At about 1.6 seconds, the power drops sharply back to zero.

Fuel cell power:

- The graph shows the time in seconds (0 to 2 seconds) on the x-axis and the power in kW (-100 to 50 kW) on the y-axis. At the beginning, the power output of the fuel cell is slightly negative. At about 0.5 seconds, there is a sudden increase in the power output, which becomes positive and stabilizes near 40 kW. After 0.5 and 1.5 seconds, the power output remains relatively stable with slight variations. After 1.6 seconds, there is an abrupt drop in power output, which stabilizes near zero, albeit slightly positive.

At 0.5 seconds, the PV system and the fuel cell begin to generate power almost simultaneously, indicating a synchronized reaction to an initial event or circumstance. Approximately 1.6 seconds later, both systems stop generating power at almost the same time, showing that the system shuts down or shuts off in a coordinated manner. The combined power output of the PV system and the fuel cell allows for a constant power supply to the load. The system shows remarkable responsiveness to variations in load demand and power generation conditions. Sudden power variations within the system involve the emulation of scenarios such as load connections or disconnections, as well as variations in solar irradiance that affect the performance of the PV panels.

The observed behavior is commonly found in simulations of hybrid power generation systems, in which the stability and responsiveness of the system to sudden variations in operating conditions and load demand are evaluated.

3.6 PV array and fuel cell energy production results

Figure 10 shows two graphs showing the power generation of a hybrid system consisting of photovoltaic (PV) panels and fuel cells over a period of time. Subsequently, a detailed analysis of the results shown in the graphs is presented below.

The graphs presented illustrate the advantages and limitations of photovoltaic panels and fuel cells. A thorough examination of these findings is essential for

developing sustainable energy systems that optimize the efficiency and stability of electricity supply by leveraging each technology's advantages and addressing its shortcomings.

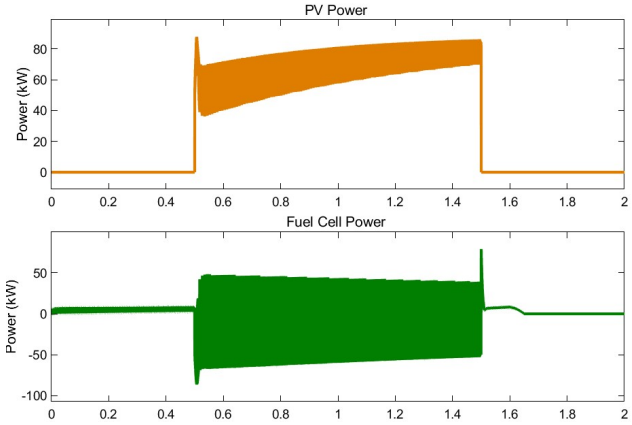

Fig. 10: Load demand of PV Array

PV Power:

- The graph shows the x-axis indicating the time in seconds (0 to 2 seconds) and the y-axis representing the power output in kilowatts (0 to 100 kW). Initially, the power output of the solar array is non-existent. At around 0.5 seconds, there is a sudden increase in the power output of the PV array, which reaches a maximum of approximately 25 kW. Between 0.5 and 1.5 seconds, the output power of the PV system gradually increases to about 85 kW. Subsequently, after 1.6 seconds, there is a sudden decrease in the power output to zero.

Fuel Cell Power :

- The graph illustrates the x-axis representing time in seconds (from 0 to 2 seconds) and the y-axis representing power in kilowatts (from -100 to 50 kW). Initially, the fuel cell generates slightly negative power. At about 0.5 seconds, there is a sudden increase in power, which reaches a maximum of about 40 kW. Between 0.5 and 1.5 seconds, the fuel cell power remains relatively stable, with small variations, hovering around 40 kW. After 1.6 seconds, there is a sudden decrease in power output, which eventually stabilizes at zero.

At 0.5 seconds, both the PV and fuel cell begin to generate power almost simultaneously, suggesting a coordinated response to a start-up event or condition. At about 1.6 seconds, both systems stop generating power almost simultaneously, indicating a coordinated shutdown or system shutdown. The combination of the power generated by the PV and fuel cell allows for a stable power supply, showing good responsiveness to changes in load demand and generation conditions. Abrupt changes in power suggest the simulation of events such as load connection or disconnection or variability in solar irradiance for the PV panels.

The observed behavior is commonly observed in simulations of hybrid power generation systems, where the stability and responsiveness of the system to sudden variations in operating conditions and load requirements are evaluated.

4 Discussion

Analysis of the results illustrates the dynamic behavior of a microgrid incorporating photovoltaic generation and a fuel cell in response to changing load demands. The PV system generates increasing amounts of power with increasing solar irradiance, stabilizing at a high level to meet most of the demand during periods of maximum solar irradiance. In cases where the PV system's power output is insufficient to meet the load demand, the fuel cell turns on and modulates its power output to make up the shortfall, as shown in the figures opposite. This behavior means that both systems are effectively synchronized and that the transition to electricity supply is smooth, with minimal impact from load fluctuations. This highlights the effectiveness of the implemented control strategy, which ensures a continuous and stable power supply to the microgrid even with fluctuations in PV generation and load demand.

5 Conclusion

Simulation provided by Matlab/Simulink software was used for the implementation. Data acquired from a dynamic generation model including a PV panel and a fuel cell were used for this purpose. Different voltage, current and power behaviors were observed in these two devices as a function of solar PV absorption. These parameters are incorporated into a consumption model of 6 kW for the fuel cell and 85.2 kW for the PV panels. The whole process was carried out using energy conversion methodologies. Consequently, it is feasible to state that the integration of hybrid power generation is practical for large-scale deployment, marking an important milestone to enable and ensure the utilization of clean energy consumption.

In analyzing all of the results obtained, there is clear documentation of the operational functionality of the hybrid generation system, facilitated by the inclusion of the PEM cell that provides the system with a reliable energy reserve. It is evident that the performance and efficiency of the system will be

influenced by the solar irradiance experienced during specific time periods.

However, any energy shortfall will be supplemented by a backup system and an energy storage mechanism that encompasses both hydrogen and battery systems. A noticeable decrease in the energy supplied to the system will trigger a systematic energy cycle, as demonstrated by system load management, culminating in a sustainable and efficient operational framework.

Acknowledgment:

I would like to express my sincere thanks in the preparation of my article to Engineers Jessica Castillo and Carlos Quinatoa, who were my guides in this process. To the research assistant Luis Camacho for his support and guidance, which were fundamental for the success of this work. I am grateful for the time, patience and knowledge he has shared. I sincerely appreciate his generosity and professionalism. My sincere thanks to all.

Declaration of Generative AI and AI-assisted Technologies in the Writing Process

While preparing this work, the authors used Grammarly to edit the language. After using this service, the authors reviewed and edited the content as needed and took full responsibility for the content of the publication.

References:

[1] The environmental impact of renewable energy. *International Journal of Business Economic Development*, 11(01), 2023.

[2] S Gkalonaki and K Karatzas. Assessing the environmental impacts of renewable energy sources with emphasis on wind energy. *IOP Conference Series: Earth and Environmental Science*, 1123(1):12053, 2022.

[3] Oriza Candra, Abdeljelil Chammam, José Ricardo Nuñez Alvarez, Iskandar Muda, and Hikmet Ş Aybar. The Impact of Renewable Energy Sources on the Sustainable Development of the Economy and Greenhouse Gas Emissions. *Sustainability*, 15(3):2104, 2023.

[4] Tunji John, ; Oladebeye, Dayo Hephzibah, ; Adesusi, Olanrewaju Moses, ; Oni, and Peter Bamidele. Environmental Impact of Renewable Energy Sources: Wind and Solar. Number August, Ado Ekiti, Nigeria, 2019.

[5] Rakesh Kumar Parida. PEM Fuel Cell based PV/Wind Hybrid Energy System. In *2022 OPJU International Technology Conference on Emerging Technologies for Sustainable Development (OTCON)*, pages 1–6, Raigarh, Chhattisgarh, India, 2023. IEEE.

[6] Noemi Tatiana Quishpi Chasiluisa, Sonnia Marisol Miranda Sánchez, Rafael Alexander Córdova Uvidia, and Magdy Mileni Echeverría Guadalupe. Renewable Energy Integration for Vehicles: Solar Energy and Green Hydrog. *ESPOCH Congresses: The Ecuadorian Journal of S.T.E.A.M.*, 2(2):611–622, 2022.

[7] Jithu Raj and S R Rajasree. A Microgrid with Hybrid Solar - Fuel Cell System With CHP Application. In *2022 IEEE 2nd International Conference on Sustainable Energy and Future Electric Transportation (SeFeT)*, pages 1–6, Hyderabad, India, 2022.

[8] Xiaomin FANG and Xiaolu LI. Design and Simulation of Hybrid Thermal Energy Storage Control for Photovoltaic Fuel Cells. *Thermal Science*, 27(2):1031–1039, 2023.

[9] Hemant Sharma, Akhil Nigam, and Kaml Kant Sharma. Modeling & Simulation Analysis of Solar PV System Using MPPT Controller for Study of Hybrid Energy System. In *2023 Fifth International Conference on Electrical, Computer and Communication Technologies (ICECCT)*, pages 1–6, Erode, India, 2023. IEEE.

[10] R Sagayaraj, S Priya, S Malathi, and S Sujith. IoT Monitoring for Hybrid Photovoltaic Fuel Cell System. In *2023 International Conference on Sustainable Computing and Smart Systems (ICSCSS)*, pages 949–953, Coimbatore, India, 2023. IEEE.

[11] Wasin Pirom and Anuchart Srisiriwat. Experimental Study of Hybrid Photovoltaic-PEM Electrolyzer-PEM Fuel Cell System. In *2022 International Electrical Engineering Congress (iEECON)*, pages 1–4, 2022.

[12] Mubaarak Saif, Delong Zhang, Longze Wang, Menghwar Mohan, Manoj Panjwani, Cai Li, Yan Zhang, and Meicheng Li. Efficient photovoltaics-integrated hydrogen fuel cell-based hybrid system: Energy management and optimal configuration. *Journal of Renewable and Sustainable Energy*, 13(1):13502, 2021.

[13] Ayad T Abdulhafedh, Alaa Ali, Layth A.Jasim, and Hassan Gheni. A stand-alone hydrogen photovoltaic fuel cell hybrid system for efficient

renewable energy generation. *Periodicals of Engineering and Natural Sciences (PEN)*, 10(1):557, 2022.

[14] Hany A Khater, Amr Abdelraouf, and Mohamed Beshr. Optimum Alkaline Electrolyzer-Proton Exchange Membrane Fuel Cell Coupling in a Residential Solar Stand-Alone Power System. *International Scholarly Research Notices*, 2011(1):1–13, 2011.

[15] Diego Feroldi and Marta Basualdo. *Description of PEM Fuel Cells System*, volume 87, pages 49–72. Springer London, London, 2012.

[16] Xuan Hieu Nguyen and Minh Phuong Nguyen. Mathematical modeling of photovoltaic cell/module/arrays with tags in Matlab/Simulink. *Environmental Systems Research*, 4(4):1–13, 2015.

[17] S. Sami and D. Icaza. Numerical Modeling, Simulation and Validation of Hybrid Solar Photovoltaic, Wind Turbine and Fuel Cell Power System. *Journal of Technology Innovations in Renewable Energy*, 4(3):96–112, 2015.

[18] F H Fahmy, Abd El-Shafy Nafeh, N M Ahamed, and Hanaa Farghally. A simulation model for predicting the performance of PV powered space heating system in Egypt. In *ICCCE 2010 - 2010 International Conference on Chemistry and Chemical Engineering, Proceedings*, pages 173–177, Cairo, Egypt, 2010.

[19] Pelin Yilmaz Bolat, Mehmet Hocaoglu, and Alp Konukman. A pre-feasibility case study on integrated resource planning including renewables. *Energy Policy*, 36:1223–1232, 03 2008.

[20] A. M. Abd El-Aal, J. Schmid, and J. Bard. Modelling and simulation of a stand-alone hydrogen photovoltaic fuel cell hybrid system for long-term operation. *International Journal of Modelling and Simulation*, 26(4):370–376, 2006.

[21] Jahangir Khan and M Tariq Iqbal. Dynamic modeling and simulation of a small wind-fuel cell hybrid energy system. *Renewable Energy*, 30(3):421–439, 2004.

[22] Hamideh Najafizadegan and Hassan Zarabadipour. Control of Voltage in Proton Exchange Membrane Fuel Cell Using Model Reference Control Approach. *International Journal of Electrochemical Science*, 7(8):6752–6761, 2012.

[23] M.Mahalakshmi. Modeling, Simulaton and Sizing of Photovoltaic/Wind/Fuel Cell Hybrid Generation System. In *International Journal of Engineering Science and Technology*, volume 4, pages 2356–2365, Tamilnadu, India, 2012.

[24] Samuel Sami Howard and Edwin Marín Calle. Simulation of Solar Photovoltaic, Biomass Gas Turbine and District Heating Hybrid System. *International Journal of Sustainable Energy and Environmental Research*, 6(1):9–26, 2017.

[25] J R Howell, R B Bannerot, and G C Vliet. *Solar-thermal Energy Systems: Analysis and Design*. McGraw-Hill, USA, ilustrada edition, 1982.

[26] Luis Camacho, Secundino Marrero, Carlos Quinatoa, and Carlos Pacheco. Emulation of a PEM Fuel Cell Stack from its Generic and Polynomial Model using Simulink. *WSEAS Transactions on Circuits and Systems*, 23:92–103, 2024.

Contribution of Individual Authors to the Creation of a Scientific Article (Ghostwriting Policy)

I, Fernanda Remache, am responsible for writing the initial and final version of the article after extensive research, data collection and simulation analysis.

Professors Jessica Castillo and Carlos Quinatoa were guides and were crucial in guiding this research. Luis Camacho also provided technical advice to ensure the research results. The experience and knowledge of each of them was essential to maintain ethical research standards.

Sources of Funding for Research Presented in a Scientific Article or Scientific Article Itself:
No funding was received for conducting this study.

Conflicts of Interest
The authors state that they have no financial interests or personal relationships that could affect the work done in this study.